Magnetic Compression Experiment at General Fusion

Carl Dunlea, Stephen Howard, Kelly Epp, Wade Zawalski, Alex Mossman,
Charlson Kim, Akira Hirose, and the General Fusion Team

General Fusion Inc., Burnaby, British Columbia, Canada

APS DPP Conference San Jose, California Oct. 31- Nov. 5, 2016 **CP10.00105**

INTRODUCTION

General Fusion is developing a magnetized target fusion power plant, in which implosion of a liquid lithium-lead shell by the action of pistons external to the shell will compress a compact torus to fusion conditions[1,2]. The SMRT magnetic compression experiment described in this poster was designed as a repetitive non-destructive test to study plasma physics applicable to this compression approach.

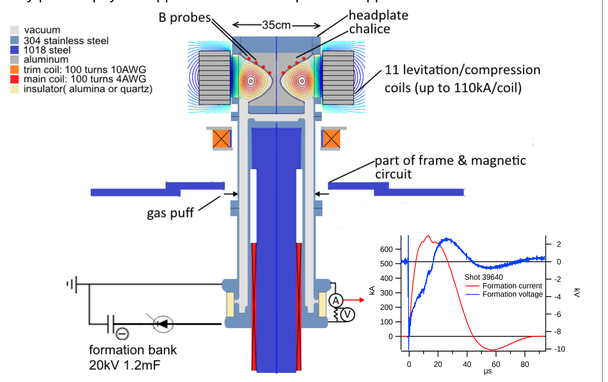

Figure 1: SMRT schematic

A spheromak compact torus (CT) is formed with a magnetized Marshall gun into a containment region with an hour-glass shaped inner flux conserver (the chalice), and an insulating outer wall. The experiment has external coils to keep the CT off the outer wall (levitation) and then rapidly compress it inwards.

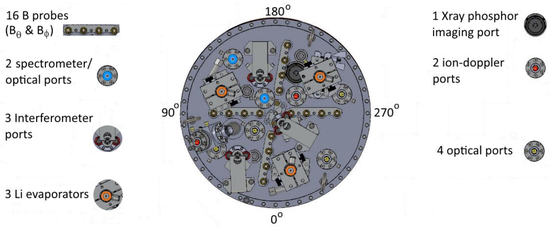

Figure 2: Machine headplate schematic indicating main diagnostics & Li gettering ports.

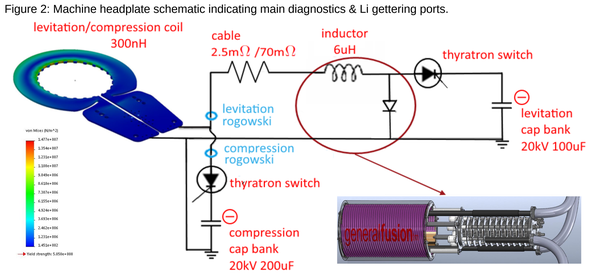

Figure 3: Levitation and compression circuit for a single-turn coil.

Each coil has a separate identical circuit. Unlike the crowbarred levitation currents, the compression currents are allowed to ring with the capacitor discharge. Peak CT compression is achieved at the peak of the first half period. Levitation and compression current profiles can be seen in figures 8, 10 & 11.

CONCLUSIONS

- Levitated CT lifetime increased by ~50% with a longer coil (i.e. 11 coils vs 6).
- Plasma impurities were a major problem with the original design (6 coils), especially with the quartz wall.
- Matching decay rates of levitation current & CT toroidal current led to increased good shot repeatability, less apparent MHD activity, and ~10% lifetime increase.
- B_θ rises by a factor of up to 9(max) / 7.5(average) on the r=26mm probes at compression, and density (r=65mm interferometer) rises by a factor of up to 7.
- Compressional flux-conservation was greatly improved with the long coil.
- Compressional asymmetry requires further study. Asymmetric shaft current diversion is associated with compressional flux conservation.

REFERENCES

1) M. Laberge, et al. *Acoustically driven Magnetized Target Fusion*, Fusion Engineering (SOFE), 2013 IEEE 25th Symposium on, pp.1-7, 10-14 June 2013; doi: 10.1109/SOFE.2013.6635495
2) P. O'Shea, et al. CP10.00103 : *Acoustically Driven Magnetized Target Fusion At General Fusion: An Overview*, 2:00 PM–5:00 PM, Monday, October 31, 2016, Exhibit Hall 1, 58th Annual Meeting of the APS Division of Plasma Physics, San Jose, California
3) Mimetic Operator-Based MATLAB 2-D Equilibrium Solver For Non-Uniform Quadrilateral Grids. C. Akcay, C. Kim, G. Marklin, R. Milroy PSI Center, University of Washington and the NIMROD Team.

ACKNOWLEDGEMENTS

Funding provided in part by University of Saskatchewan, NSERC, and MITACS, Canada

CT FORMATION INTO LEVITATION FIELD ORIGINAL CONFIGURATION (6 COILS)

- With the original design levitation field profile from 6 coils CTs were short-lived, up to ~100μs FWHM from poloidal probes at 52mm, compared with over 400μs on similar General Fusion injectors with an aluminum outer flux conserver, without levitation & magnetic compression.

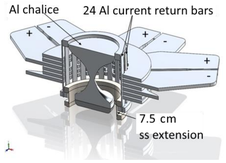

Figure 4: (a) Schematic of 6 coils

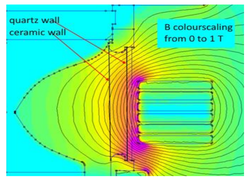

(b) FEMM model of levitation field - 6 coil set – 30kA/coil at 800Hz.

- CT lifetime was increased, up to ~160μs, by shortening the ceramic insulator by 7.5cm and adding a steel extension tube (figure 4 (a)).
- The extension mitigated the problems of sputtering of steel at the alumina/steel lower interface, and of CT radiative heat loss due to impurities being added to the plasma as a result of plasma interaction with the insulating wall, especially during the formation process.
- Increasing initial CT flux (ie increasing V_{form} and stuffing field) to the nominal levels associated with MRT CTs did not improve lifetime.

Performance drop with transition from ceramic to quartz wall:

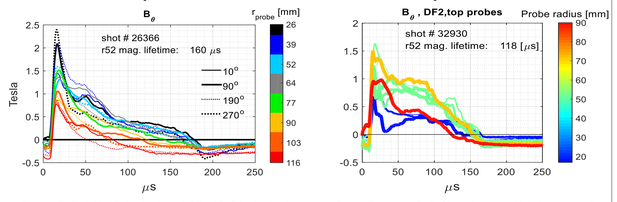

Figure 5: Poloidal B for levitated CT with 6 levitation/compression coils, ceramic (left) and quartz (right) outer wall

- An insulator with larger internal radius was experimented with (original alumina replaced with quartz).
- Although CT lifetime should scale with r^2, lifetime decreased significantly (~160μs to ~120μs) with the larger radius quartz tube, suggesting that the quartz wall led to more impurities and further cooling.
- Quartz did not have a significant benefit from lithium gettering (see fig. 9).
- Initial CT flux remained limited with the quartz wall.
- The coils are closer to the inner radius of the quartz wall, and the axial gradient of the levitation field along the wall is increased. For optimal performance, levitation field had to be increased, and stuffing flux reduced (perhaps to allow for more momentum to push aside the increased levitation field), with the quartz wall.
- This suggested that on the 6 coil setup, a levitation field that is strong enough to have partial success at keeping the CT off the wall below and above the coils is too strong to allow successful high-flux CT entry to the pot. Field would be harder to displace with a longer coil.

IMPROVED CONFIGURATION (11 COILS)

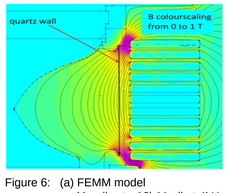

Figure 6: (a) FEMM model
11 coil set - 16kA/coil at 4kHz

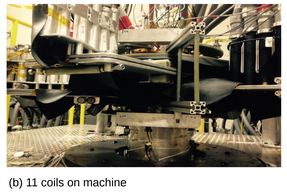

(b) 11 coils on machine

- The setup with 11 coils allowed for formation of higher-flux CTs.
- The absence of gaps outboard of the insulator above and below the coils reduced displacement of the levitation field during CT formation, leading to a reduction of plasma/insulator interaction and impurities (see fig. 7).
- CT lifetime was increased ~50%, up to ~190μs, with 11 coils despite the unfavorable quartz wall. It is expected that lifetime would increase to over 300μs with a setup with 11 coils on a quartz-radius ceramic wall.

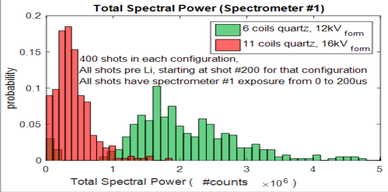

Figure 7: Even at increased formation voltage, total spectral power (verified by optical data) is ~4 times lower with 11 coils.

Levitation field decay rate affects performance:

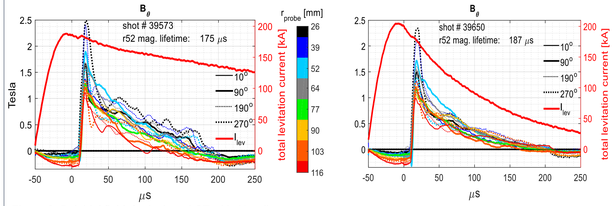

Figure 8: Poloidal field for levitated CT with 11 coils
(a) with 2.5 mΩ cables (b) with 70 mΩ cables

- Adding resistance to the circuit between the main inductors and the coils (figure 2) helped match the decay rate of B_{lev} to that of the CT.
- This improves on the 'low level compression' situation in which a nearly constant levitation flux pushes on a CT which has rapidly decreasing flux.
- A much higher rate of 'good' shots, smoother decays of B_θ & B_ϕ (less apparent MHD activity), and a ~10% increase in lifetime, was observed with the 70 mΩ cables.

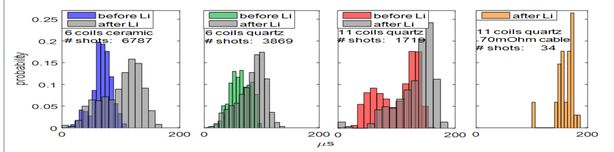

Figure 9: Pre-lithium CT lifetimes were better with the ceramic wall despite the smaller volume. Lithium gettering was very effective on the ceramic wall, not so effective on quartz.

- The 'double-gaussian' shape for 11 coils (before Li, 3rd subfigure) may be due to the ~35% of shots taken in suboptimal machine-parameter space (ie values of V_{form}, V_{lev}, V_{comp}, I_{main}, & gaspuff) that were rapidly explored in new configurations such as without levitation inductors, and with passive or open-circuited coils.

CT COMPRESSION

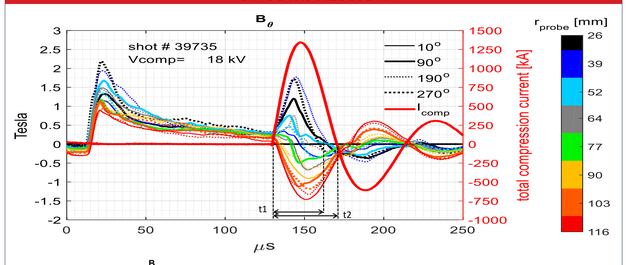

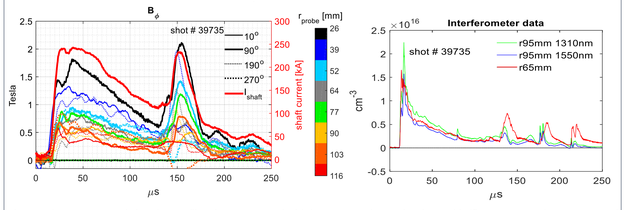

Figure 10: B_θ, B_ϕ, and density profiles for an example high-compression ratio shot, with 'flux conservation parameter' ~0.7. The flux conservation parameter is t1 / t2, where t1 is the average time (over the 2 probes 180° apart at 26mm) from the start of the compression pulse to the time at which the measured B_θ falls to 0, and t2 is half-period of the compression current.

- B_θ rises by a factor 9.1(max) / 7.5(avg), r=26mm probes, at compression, & density (r=65mm interferometer) rises by a factor of 7 (shot #39735).
- Density front generally moves in at 5 to 10 km/sec on compression shots.
- Rise of B_ϕ at compression (lower left subfigure above) indicates partial diversion of crowbarred shaft current path from external bars (see fig 4a) to plasma around the CT (see fig 12) .

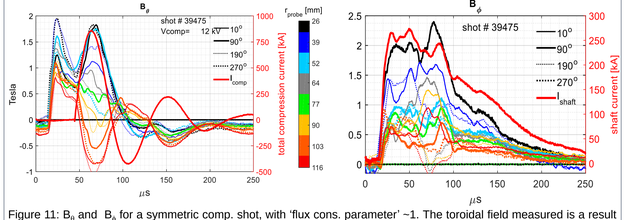

Figure 11: B_θ and B_ϕ for a symmetric comp. shot, with 'flux cons. parameter' ~1. The toroidal field measured is a result of crowbarred shaft current. Fluctuations in B_ϕ, which generally peak ~5μs after maximum compression on many shots, indicate more diversion at preferred toroidal angles. In this shot, I_{shaft} diverts primarily at ~190 degrees (see fig. 2).

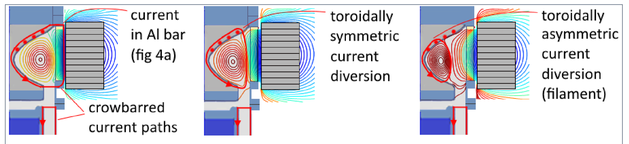

Figure 12: After the 50μs formation capacitor-driven pulse, crowbarred current continues to flow in 2 separate current loops as indicated. External poloidal current, and B_ϕ at probes, rise at compression as the current path shifts to a lower inductance one (central subfigure). Asymmetric current filaments (right subfigure) may explain the dip in B_ϕ that is observed at one toroidal angle on many compression shots (eg see Figure 11).

- Asymmetric current diversion was also usual towards the end of CT life on levitation-only shots with the low resistance levitation circuit (low level compression - fig 8a), but was not observed on levitation-only shots with the 70 mΩ cables.
- Flux-conserving compression shots generally exhibit more asymmetric current diversion than non flux-conserving shots.
- As the CT decompresses, the current path returns towards its pre-compression path.
- Several shots with ~1ms of sustained ~90kA capacitor-driven shaft current have clear n-odd fluctuations in B_θ.

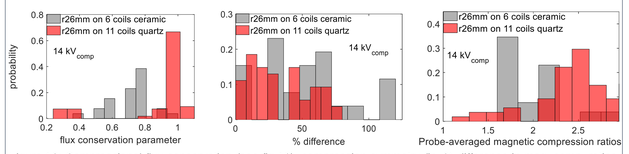

Figure 13: Compressional flux conservation (see fig 10), compression symmetry (ie. % difference in mag. comp. ratios at the 2 probes 180° apart at r=26mm), and magnetic compression ratios, were improved with the 11 coil configuration. All data shown here is from shots with compression fired 40-60μs after formation, and at moderate V_{comp} (14kV) because that was the setting usually used with 6 coils.

- Vastly improved compressional flux conservation with 11 coils may be due to the field profile (see figs 4b, 6a) as well as impurity reduction.

EQUILIBRIUM CODE RESULTS

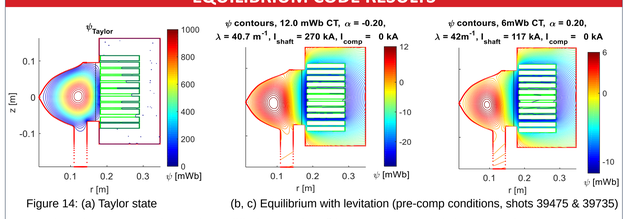

Figure 14: (a) Taylor state (b, c) Equilibrium with levitation (pre-comp conditions, shots 39475 & 39735)

- A mimetic operator-based equilibrium solver[3] is used to model the experiment.
- Assumes the linear dependence $\lambda(\psi) = \bar{\lambda}(1 + \alpha(2\tilde{\psi} - 1)$, an iterative algorithm solving $\psi_{n+1} = -(\Delta^*)^{-1}[\bar{\lambda}(1+\alpha(2\tilde{\psi}-1))]\psi + \mu_0 I_{shaft}/2\pi] + 2\pi^2(\frac{I_{shaft}}{\pi_{area}})^2\beta']_n$
- Code modified to allow deletion of areas in the mesh that correspond to irregular features of the machine geometry such as the levitation/compression coils.
- FEMM is used to get boundary values of ψ corresponding to the currents and frequencies associated with dc main coil current & levitation/compression coil currents.
- Boundary values are superimposed on the interior (coils) and exterior boundary points.

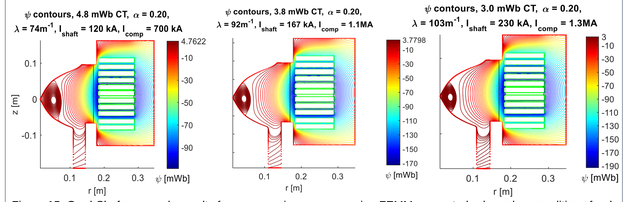

Figure 15: Grad-Shafranov code results for compression ramp-up using FEMM-generated ψ boundary conditions for dc main coil (70A) , levitation (4kHz, ~80kA total at 130us, just before start of compression), and compression fields (10kHz), corresponding to those in shot #39735 (see fig. 10). Shaft current is ramped up along with compression ψ_{bc}.

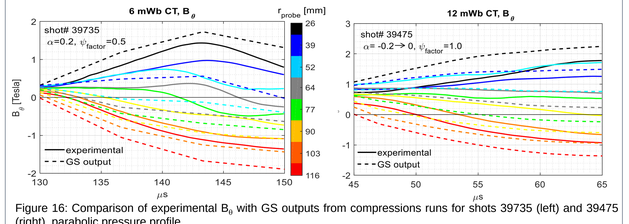

Figure 16: Comparison of experimental B_θ with GS outputs from compressions runs for shots 39735 (left) and 39475 (right), parabolic pressure profile.

ψ_{factor} is the factor by which $\psi_{magnetic\ axis}$ is scaled over the 20μs compression pulse. A reasonable match to experimental data can be found by setting ψ_{factor} = 0.5 (half flux lost during the pulse) for #39735, and = 1 (no flux lost) for #39475. These shots have measured flux conservation parameters of 0.7 and 1 respectively (see figures 10 & 11). This indicates that the measured 'flux conservation parameter' is indeed an indication of compressional flux conservation.